PNAS

Main Manuscript for

Evidence for a Metal–Bosonic Insulator–Superconductor Transition in Compressed Sulfur

Kui Wang[a,b,c], Hongjian Zhao[b], Guangtao Liu[b], Mi Zhou[b], Yinqi Chen[a,b], Qiushi Li[a,b], Guangchen Ma[a,b], Hongbo Wang[a,b,*], Russell J. Hemley[c,d,e,*], Yanming Ma [a,b,f,*]

[a]State Key Laboratory of Superhard Materials, College of Physics, Jilin University, Changchun 130012, China; [b]Key Laboratory of Material Simulation Methods and Software of Ministry of Education, College of Physics, Jilin University, Changchun 130012, China; [c]Department of Physics, University of Illinois Chicago, Chicago, IL 60607, USA; [d]Department of Chemistry, University of Illinois Chicago, Chicago, IL 60607, USA; [e]Department of Earth and Environmental Sciences, University of Illinois Chicago, Chicago, IL 60607, USA; [f]International Center of Future Science, Jilin University, Changchun 130012, China.

[*]Corresponding authors: Kui Wang, Hongbo Wang, Russell J. Hemley, Yanming Ma.

Email: kuiwang2@uic.edu; whb2477@jlu.edu.cn; rhemley@uic.edu; mym@jlu.edu.cn

Author Contributions: H.W. conceived and designed the project; K.W., G.L., M.Z., Y.C., Q.L., and G.M. carried out the experiments; K.W., H.Z., H.W., R.J.H., and Y.M. performed data analysis and interpretation of the results; K.W., H.W., R.J.H., and Y.M. wrote the paper with input from all authors.

Competing Interest Statement: The authors declare no competing interests.

Classification: Physical Sciences, Physics

Keywords: High pressure; superconductivity; bosonic insulator; diamond anvil cell

This PDF file includes:

Main Text

Figures 1 to 5

Abstract

The abrupt drop of resistance to zero at a critical temperature is the paradigm of the metal–superconductor transition. However, the emergence of an intermediate bosonic insulating state characterized by a resistance peak preceding the onset of the superconducting transition has challenged traditional understanding. Notably, this phenomenon has been predominantly observed in disordered or chemically doped low-dimensional systems, raising intriguing questions about the generality of the effect and its underlying fundamental physics. Here, we present a systematic experimental study of compressed elemental sulfur, an undoped three-dimensional (3D) high-pressure superconductor, with detailed measurements of electrical resistance as a function of temperature, magnetic field, and current. The anomalous resistance peak observed in this 3D system is interpreted based on an empirical model of a metal–bosonic insulator–superconductor transition, potentially driven by vortex dynamics under magnetic field and energy dissipation processes. These findings offer a fresh platform for theoretical analysis of the decades-long enigmatic of the underlying mechanism of this phenomenon.

Significance Statement

The metal–bosonic insulator–superconductor transition, predominantly observed in low-dimensional systems with disorder or magnetic impurities, defies mean-field theory and challenges the long-held picture of a straightforward transition from metal to either superconductor or insulator. Here, we report experimental evidence of a magnetic field-tuned bosonic insulating state in compressed 3D sulfur in the vicinity of its superconducting transition. The experiments reveal a prominent, and apparently unprecedented, concurrent resistance peak as a function of temperature, magnetic field, and current in the same superconductor. The results suggest the potential for revealing diverse electronic and transport phenomena in putatively simple systems and open new avenues for advancing the understanding of the underlying physics.

Main Text

Introduction

Quantum mechanics dictates that bosons created from two paired electrons either condense into a macroscopic superconducting state with zero resistance or localize into an insulating state with infinite resistance (1), a scenario that aligns with a *metal–superconducting transition* (MST) and *metal–insulator transition* (MIT) as temperature goes down, respectively. The puzzling observation, however, is the *metal–bosonic insulator–superconductor transition* (MIST) identified by the resistance peak situated in the vicinity of the superconducting critical temperature (T_c) on the resistance-temperature (R-T) curve (2). This anomalous change in resistance is predominantly observed in low-dimensional materials, such as 1D wires and whiskers (3,4), thin films (5-9), and quasi-two-dimensional cuprates (10-14), where the resistance peak can typically reach tens to hundreds of percent above the residual resistance close to T_c. The surprising emergence of the excess resistance violates mean-field theory (15) and upends long-held wisdom about the routine manifestation of the direct transition from metal to superconductor or insulator.

Since the discovery of this anomalous resistance behavior in 1950s (2), a significant amount of effort has been devoted to probing the origin of the unusual $R(T)$ peak, and an eclectic set of models have been proposed to understand this phenomenon. These include superconducting–normal boundaries, disorder and fluctuations, vortex dynamics and Josephson coupling in layered systems, nonequilibrium superconductivity near phase slip centers, charge imbalance, and competition between superconducting and insulating states in 2D systems (2,3,5,7,11,16-22). These models and theories, however, generally invoke or require some aspect of the reduced dimensionality of the systems investigated, for example, 2D thin film,1D whiskers, and wires. While a few experimental studies have been conducted on 3D systems (23-25), the observed resistance peaks have amplitudes that are relatively small [*e.g.*, <6% for Cu-Zr alloys (23,24)], which may be attributed to weak localization effects. On the other hand, resistance peaks as high as 1600% have

been reported for boron-doped diamond (25), which surpasses the range expected for weak localization. However, disorder and granularity in the material may also contribute to the resistance peak, which complicates understanding the underlying mechanism. Due to the diversity of samples and experimental configurations for these measurements, it is unclear how (and if) the various observations are related. Therefore, the quest for additional information in well-defined 3D material systems is crucial for uncovering universal explanations.

In this work, we find that highly compressed bulk sulfur, which has the highest T_c among non-metallic elements (26), exhibits a robust magnetic field-induced MIST, evidenced by an anomalous resistance peak that appears prior to the onset of the superconducting transition. The amplitudes of $R(T)$ and $R(H)$ peaks both reach a maximum of approximately 158% larger than the normal-state resistance (R_n) at 165 GPa. Further, resistance-current (R-I) curves under magnetic field also reveal anomalous peaks. Notably, our study thus represents the first instance of the concurrent observation of a prominent resistance peak as a function of temperature, magnetic field, and current in the same superconductor. The findings for compressed sulfur, a well-established elemental superconductor, suggest the possibility of unveiling diverse electronic and transport phenomena in putatively simple systems and open avenues for further delving into the essence of anomalous transport mechanisms in condensed matter.

Results

Pressure-induced superconductivity in sulfur under pressure has been the subject of significant attention since its discovery in 1997 (26). A critical temperature of 10 K at 93 GPa rising to 17 K at 162 GPa was originally reported using magnetic susceptibility measurements (26). The results were subsequently confirmed by combined electrical resistance and magnetic susceptibility to 230 GPa, with the T_c dropping to 15 K at the highest pressure (27). Discrepancies in the pressure dependence of T_c between theoretical predictions and experimental observations as well as among different experimental studies have been noted (26-29). These discrepancies, as well as deeper questions about the nature of the transition motivated the present extended experimental study using in particular detailed measurements as a function of high magnetic field.

We observed pressure-induced superconductivity evidenced by the emergence of zero resistance in the R-T curves measured from 93 to 196 GPa (Fig. 1*A*), which is broadly consistent with previous work. Notably, a broadened resistance drop was observed at 119 GPa and 136 GPa, possibly resulting from the gradual transition from the body-centered orthorhombic (bco) S-IV to the β-Po S-V phase. Above 155 GPa, the superconducting transition curves steepened, signifying the complete entry of the sample into the S-V phase, in agreement with the phase transition pressure reported in previously (30). Comparison of our data with those from previous experiments and theoretical calculations (Fig. 1*B*) reveals that the T_c measured in the S-IV phase is higher than previous results, whereas a gradual decline in T_c is observed in the S-V phase, in agreement with both the original results (26,27) and theoretical calculations (29).

Resistance curves as a function of temperature at different external magnetic fields of sulfur in cell_2 at 163 GPa are illustrated in Fig. 2*A*. When the temperature drops below T_c, the zero-field resistance curve exhibits a standard sharp transition from the normal metal to the superconducting state, consistent with the traditional transport picture (31). However, the introduction of an external magnetic field results in a distinct change in resistance behavior. At a magnetic field of 0.1 T, the superconductivity $R(T)$ onset shifts to the lower temperature and is accompanied by a small rise preceding the superconducting transition before dropping to the zero-resistance state. Upon increasing the field to 0.3 T, the resistance peak becomes much more conspicuous, up to 119% larger than R_n, and then the resistance did not reach zero on cooling to 2 K. The amplitude of the resistance peak continued to increase with field, reaching 131% at 0.4 T, with no observable decrease in resistance at the low-temperature limit of the experiment. Beyond 0.4 T, on the other hand, the resistance peak gradually decreased, ultimately resembling metallic behavior throughout the temperature range above 2 T. This giant $R(T)$ peak is an established hallmark of a MIST (25).

The $R(T)$ peak behavior in response to the magnetic field suggests that the resistance jump caused by the disruption of superconductivity by the magnetic field will be followed by a regime of negative magnetoresistance, implying that the $R(H)$ curves will also exhibit a resistance peak. To

present this anomalous behavior more clearly, we measured the magnetoresistance of the same sample in cell_2 at different temperatures, as depicted in Fig. 2*B*. The *R*(*H*) curve measured at 2 K (orange) demonstrates a transition from the zero resistance to a non-zero state with a rapid rise in resistance as the magnetic field increases, peaking at ~0.32 T. This behavior is consistent with the typical destruction of the superconducting state by a magnetic field. Subsequently, the sample exhibits a period of remarkable negative magnetoresistance until about 2 T, after which it behaves in line with the response of a normal metal to the magnetic field. The peak was observed to decrease continuously with the increasing temperature, diminishing from 91% at 2 K to completely disappearing at 19 K. Moreover, the position of the peak exhibited a shift towards the low-field region with increasing temperature. The results obtained from this measurement indeed align with the phenomenon observed during the resistance measurement of cooling cycles. Similar results were observed in cell_3 of S-V phase at 165 GPa (*SI Appendix*, Fig. S1), where both the *R*(*T*) and *R*(*H*) peaks were up to around 158%. In the S-IV phase we also observed *R*(*T*) and *R*(*H*) peaks of approximately 9% in cell_6 at 117 GPa (*SI Appendix*, Fig. S2). The arrangement of the electrical leads has been reported to affect the strength of the resistance peak in metallic glasses [24]. Experimental constraints of the diamond anvil cell precluded direct tests of this effect in high-pressure sulfur, but we point out that the strong resistance peak was observed in multiple experiments having slight differences in the arrangement of the electrodes. This transport behavior offers compelling experimental evidence for a MIST in compressed sulfur.

In Glazman's theory the peak value could only be observed experimentally within a specific range of currents between an upper and a lower threshold (32). The results shown in Fig. 3*A* illustrate that the value of the current significantly influences the *R*(*H*) peak. With increasing current from 0.0005 A to 0.001 A, a slight increase in the peak resistance value is observed, indicating the presence of a lower critical current. However, when the current was further increased from 0.001 A to 0.03 A, the value of the resistance peak exhibited a significant suppression that was confirmed in various experiments (Fig. 3*B*), indicating the presence of an upper critical current. Unfortunately, the noise in the resistance measurements under magnetic field is enhanced at these low current levels, so we unable to collect useful data with further reduction of current. Additionally, increasing the current can damage the sample or the electrodes, so measurements at higher currents were also not conducted. Furthermore, our measurements consistently revealed a decrease in the magnetic field value at which the resistance peak occurred as the current increased. This shift is likely due to critical-current effects.

The current-voltage (*I*-*V*) curve serves as an important means for investigating the transport properties of materials. In a normal metal, the *I*-*V* relation is linear and passes through the origin, indicating that the resistance remains constant with varying current (Ohm's law). The suppression of the magnetoresistance peak by the current suggests the presence of an anomalous region where resistance decreases with increasing current. Fig. 4 illustrates representative *I*-*V* and *I*-*R* curves at selected magnetic fields for cell_2. The zero-resistance state is maintained as the current is increased from 0.0001 A to 0.1 A in the absence of the field, but it is disrupted when the current reaches ~0.0046 A at an external magnetic field of 0.2 T (Fig. 4*A*). These results show a distinguishing feature of superconductors, wherein superconductivity disappears above upper critical current. The above features are consistent with the response of conventional superconductivity to changes in electrical current. Upon increasing the external magnetic field to 0.4 T, an anomalous *R*(*I*) peak emerges at about 0.0017 A, exhibiting a negative rate of change at higher current values, thereby deviating from the behavior of a conventional metal but resembling that of an insulator (Fig. 4*B*). Our measurements at 2 K reveal an unconventional trend in the *R*(*I*) curve over a specific range of magnetic fields, likewise showing the observation of the anomalous peak. With increasing magnetic field, the magnitude of the peak value also grows to a maximum value before gradually decreasing. When the magnetic field exceeded 2 T, the curve gradually leveled off, indicative of the material entering a normal metal state. Similar behavior was also observed in cell_5 (*SI Appendix*, Fig. S3).

The temperature-magnetic field (*T*-*H*) phase diagram in Fig. 5 captures the sequence of transitions documented here and the overall results of our study. The superconducting state (yellow region) with zero resistance can only be sustained in the low-field region (less than 0.28 T). As the magnetic field strength increases, the material undergoes a transition from the resistance drop region (purple region) to a notable insulating state (red region), eventually evolving into a normal

metallic state (blue region) when the external magnetic field reaches a sufficiently high level. This phase diagram represents a significant departure from that of traditional 3D systems, in which a superconductor transforms directly to a normal metal at high external magnetic fields.

Discussion

The disparate observations of similar resistance peaks in $R(T)$ and/or $R(H)$ measurements of superconductors have prompted the question of a common origin for this phenomenon. Our observation of dramatic combined effects of T, H, and I on the resistance peak in superconducting sulfur, including the giant enhancement as well as suppression of the peak as a function of external variables, suggests that this simple 3D superconductor is a key candidate for investigating the underlying mechanism. We demonstrate that the formation of a bosonic insulator mainly based on the increase of resistance preceding the superconducting transition, which has been experimentally confirmed [33] and widely recognized in low-dimensional or disordered superconducting systems [1,34-37]. At this stage, electrons begin to form Cooper pairs but become localized, effectively removing fermions from electrical transport and substantially increasing the sample's overall resistance [37-39].

Previous studies indicated that the introduction of disorder plays a pivotal role across various scenarios, e.g., regulating thin film sample thickness (17), doping superconducting systems with magnetic elements (23,24), or constructing granular metal systems (25). It has been suggested that the granularity-correlated disorder in heavily boron-doped diamond results in the formation of islands that can trap Cooper pairs at sufficiently low temperatures and subsequently diminish the carrier density in the material, thus giving rise to an intermediate bosonic insulating state (25). The effect of intrinsic disorder can be largely ruled out for crystalline elemental sulfur. Moreover, the steepness of the T_c resistance drop at zero field (approximately 1 K wide) is also consistent with ordered, homogeneous samples.

Our experimental data suggest that application of an external magnetic field is necessary for the emergence of the anomalous resistance peak. For type-II superconductors, applying a magnetic field within the range between the lower critical field (H_{c1}) and the upper critical field (H_{c2}) induces vortices within the superconductor. The number of vortices increases with the magnetic field, which it may also cause vortex shifting or motion. In earlier discussions, vortex motion was proposed as a possible mechanism candidate (40); however, the predicted magnitude of the transverse peak was orders of magnitude smaller than the observations. Subsequent in-depth investigations of vortex dynamics demonstrated that various factors, such as the external magnetic field's influence and the micropattern of the sample, lead to significant alterations in the configuration and transition of vortices, resulting in substantial energy dissipation (19,31,41). The Bardeen-Stephen model has been employed to elucidate the energy dissipation in moving vortices within bulk systems (41). According to this model, the vortex is assumed to be the normal-state core within the coherence length for simplification. The electric field caused by the moving vortex is proportional to the velocity of the vortices and the number of vortices. Therefore, the energy dissipation increases with current and magnetic field. This theoretical framework may serve as a starting point for explaining our findings, but understanding the underlying mechanism will require a more in-depth theory. Exploring the dynamics of vortices under magnetic fields and delving into the mechanisms governing energy dissipation stemming from vortex dynamics could shed light on the presence of this anomalous behavior.

In conclusion, we have documented a giant enhancement of electrical resistance above T_c induced by applying a magnetic field in superconducting elemental sulfur. With increasing applied magnetic field, the $R(T)$ begins to show an anomalous resistance peak above T_c. The peak rises with field and then is progressively suppressed at a critical magnetic field of ~0.4 T, eventually disappearing completely, signaling the collapse of the insulating state. Moreover, the width of the resistance peak is enhanced with increasing magnetic field. The dramatic enhancement of the $R(T)$ peak can be interpreted as a result of a sequence of transitions from metal to bosonic insulator to superconductor on cooling. The observation of this transition sequence in undoped simple elemental solid offers a favorable material platform for in-depth exploration of the physical influence parameters and underlying mechanisms of this behavior. The results indicate that similar effects

that have been reported are not limited to low-dimensional systems. We suggest that the resistance enhancements should be evident in other 3D systems, although the phenomenon remains to be fully explained. Further theoretical and experimental studies are needed to explore the interplay of vortex dynamics and energy dissipation, as well as possible competing electronic or structural orders, are essential to elucidate the emergence of the resistance peak in compressed sulfur.

Materials and Methods

For electrical transport measurements, we utilize nonmagnetic BeCu or NiCrAl alloy diamond anvil cell (DAC) and steel DACs in experiments with and without a magnetic field, respectively. Anvil culets with different sizes were employed, depending on the required maximum pressure of the measurements. Details regarding the cells are provided in *SI Appendix*, Table S1. The sulfur powder with a purity of 99.5% (Tianjin Xintong Fine Chemical Co., Ltd) was used. The ambient-pressure Raman and x-ray diffraction measurements indicate the absence of other impurities in the sample (*SI Appendix*, Fig. S4). DAC gaskets made from nonmagnetic rhenium were used with a mixture of aluminum oxide and epoxy inserts to confine the sample, and no pressure-transmitting medium was used. Given the stability of elemental sulfur in air, samples were loaded under ambient conditions. The pressure was determined at room temperature using the diamond Raman edge scale (42), a widely utilized method in high-pressure experiments. The electrical resistance was measured using a four-probe van der Pauw configuration (43). The current used in all resistance measurements was in the range of 10^{-5} to 10^{-2} A. Currents exceeding 0.03 A were only applied only during *I-V* curve measurements, as such high currents were not sustained for extended periods during testing. The magnetic field was applied along the DAC load axis, *i.e*., perpendicular to the surface of the disk-shaped sample in the cell.

The small initial resistance of sulfur samples with thicknesses greater than 5 μm causes resistance instabilities with increasing magnetic field that can drown out the resistance change, rendering it ineffective for analysis. To address this issue, it was crucial to limit the thickness of the samples to <5 μm in our experiments under external magnetic field. Furthermore, in high-pressure experiments where the sample cavity thickness is small, there is a risk of diamond breakage at high pressures. In order to obtain high-quality resistance data while ensuring the integrity of the diamond anvils at the highest pressures, we utilized a stacking method involving the sulfur sample and insulating powder used in gasket preparation to control the sample cavity thickness (*SI Appendix*, Fig. S5). Despite the fact that the electrode only makes contact with the sulfur sample, and the sample is not expected to react with the insulating material in a high-pressure setting, there are concerns that the insulating material could influence the characteristic properties of measured sample. To eliminate this potential impact, we conducted multiple experiments in which the chamber was filled with only thin sulfur samples; consistent results were obtained that ruled out reactions with the insulating material (*SI Appendix*, Fig. S3 and Fig. S6). The calculation formula for the peak height follows the common approach in this field: subtracting R_n from R_p (resistance peak value) and then dividing by R_n. For the $R(T)$ peak, the resistance at 30 K is used as R_n, while for the $R(H)$ peak, the resistance at 2 T is taken as R_n.

Acknowledgments

This research was supported by the National Natural Science Foundation of China (Grant Nos. 52288102, 52090024, 12374007, 12474011, and 12474010), National Key R&D Program of China (Grant No. 2023YFA1608900), the Strategic Priority Research Program of Chinese Academy of Sciences (Grant No. XDB33000000), and the U.S. National Science Foundation (Grant No. DMR-2104881).

References

1. P. W. Phillips, Free at last: Bose metal uncaged. *Science* 366, 1450–1451 (2019).
2. T. G. Berlincourt, Hall effect, resistivity, and magnetoresistivity of Th, U, Zr, Ti, and Nb. *Phys. Rev.*114, 969-977 (1959).

3. P. Santhanam, C. C. Chi, S. J. Wind, M. J. Brady, J. J. Bucchignano, Resistance anomaly near the superconducting transition temperature in short aluminum wires. *Phys. Rev. Lett.* 66, 2254-2257 (1991).
4. Y. Tajima, K. Yamaya, Giant resistivity anomaly on the superconducting transition in $TaSe_3$. *J. Phys. Soc. Jpn.* 53, 495-498 (1984).
5. A. D. C. Grassie, D. B. Green, Transition anomalies of disordered aluminium films. *Phys. Lett. A* 31, 135-136 (1970).
6. S. C. Ems, J. C. Swihart, Resistance peak at the superconducting transition of thin films of tin and indium. *Phys. Lett. A* 37, 255-256 (1971).
7. H. Yamamoto, M. Ikeda, M. Tanaka, Giant resistivity anomaly in A15 Nb_3(Ge, Si) superconductive films with compositionally modulated superstructure. *Jpn. J. Appl. Phys.* 24, L314-L316 (1985).
8. P. Achat, W. Gajewski, E. Bustarret, C. Marcenat, R. Piquerel, C. Chapelier, T. Dubouchet, O. A. Williams, K. Haenen, J. A. Garrido, M. Stutzmann, Low-temperature transport in highly boron-doped nanocrystalline diamond. *Phys. Rev. B* 79, 201203(R) (2009).
9. S. Yadav, B. Gajar, R. P. Aloysius, S. Sahoo, Interplay between superconducting fluctuations and weak localization in disordered TiN thin films. *Nanoscale* 16, 20319-20330 (2024).
10. M. A. Crusellas, J. Fontcuberta, S. Piñol, Giant resistive peak close to the superconducting transition in $L_{2-x}Ce_xCuO_4$ single crystals. *Phys. Rev. B* 46, 14089-14094 (1992).
11. Y. M. Wan, S. E. Hebboul, D. C. Harris, J. C. Garland, Interlayer Josephson coupling of thermally excited vortices in $Bi_2Sr_2CaCu_2O_{8-y}$. *Phys. Rev. Lett.* 71, 157-160 (1993).
12. M. Suzuki, Resistance peak at the resistive transition in high-T_c superconductors. *Phys. Rev. B* 50, 6360-6365 (1994).
13. E. Silva, M. Lanucara, R. Marcon, Microwave surface resistance peak at T_c in $Bi_2Sr_2CaCu_2O_{8+x}$ film. *Physica C.* 276, 84-90 (1997).
14. C. Buzea, T. Tachiki, K. Nakajima, T. Yamashita, The origin of resistance peak effect in high-temperature superconductors - Apparent T_c anisotropy due to J_c anisotropy. *IEEE Trans. Appl. Superconduct.* 11, 3655-3658 (2001).
15. S. Marčelja, W. E. Masker, R. D. Parks, Electrical Conductivity of a Two-Dimensional Superconductor. *Phys. Rev. Lett.* 22, 124-127 (1969).
16. V. V. Moshchalkov, L. Gielen, G. Neuttiens, C. Van Haesendonck, Y. Bruynseraede, Intrinsic resistance fluctuations in mesoscopic superconducting wires. *Phys. Rev. B* 49, 15412-15415 (1994).
17. M. Park, M. S. Isaacson, J. M. Parpia, Resistance anomaly and excess voltage in inhomogeneous superconducting aluminum thin films. *Phys. Rev. B* 55, 9067-9076 (1997).
18. C. Strunk, V. Bruyndoncx, C. Van Haesendonck, V. V. Moshchalkov, Y. Bruynseraede, C.-J. Chien, B. Burk, V. Chandrasekhar, Resistance anomalies in superconducting mesoscopic Al structures. *Phys. Rev. B* 57, 10854-10866 (1998).
19. A. Harada, K. Enomoto, T. Yakabe, M. Kimata, H. Satsukawa, K. Hazama, K. Kodama,T. Terashima, S. Uji, Large energy dissipation due to vortex dynamics in mesoscopic Al disks. *Phys. Rev. B* 81, 174501 (2010).
20. W. J. Skocpol, M. R. Beasley, M. Tinkham, Phase-slip centers and nonequilibrium processes in superconducting tin microbridges. *J. Low Temp. Phys.* 16, 145-167 (1974).
21. K. Yu. Arutyunov, D. A. Presnov, S. V. Lotkhov, A. B. Pavolotski, L. Rinderer, Resistive-state anomaly in superconducting nanostructures. *Phys. Rev. B* 59, 6487-6498 (1999).
22. I. L. Landau, L. Rinderer, Comment on “intrinsic resistance fluctuations in mesoscopic superconducting wires”. *Phys. Rev. B* 56, 6348-6351 (1997).
23. P. Lindqvist, A. Nordström, Ö. Rapp, New resistance anomaly in the superconducting fluctuation region of disordered Cu-Zr alloys with dilute magnetic impurities. *Phys. Rev. Lett.* 64, 2941-2944 (1990).
24. A. Nordström, Ö. Rapp, Resistance-peak anomaly in metallic glasses: Dependence on currents and contact arrangement. *Phys. Rev. B* 45, 12577-12579 (1992).
25. G. Zhang, M. Zeleznik, J. Vanacken, P. W. Ma, V. V. Moshchalkov, Metal–bosonic insulator–superconductor transition in boron-doped granular diamond. *Phys. Rev. Lett.*110, 077001 (2013).

26. V. V. Struzhkin, R. J. Hemley, H. K. Mao, Y. A. Timofeev, Superconductivity at 10–17 K in compressed sulphur. *Nature* 390, 382-384 (1997).
27. E. Gregoryanz, V. V. Struzhkin, R. J. Hemley, M. I. Eremets, H. K. Mao, Y. A. Timofeev, Superconductivity in the chalcogens up to multimegabar pressures. *Phys. Rev. B* 65, 064504 (2002).
28. A. P. Drozdov, M. I. Eremets, I. A. Troyan, V. Ksenofontov, S. I. Shylin, Conventional superconductivity at 203 kelvin at high pressures in the sulfur hydride system. *Nature* 525, 73-76 (2015).
29. M. Monni, F. Bernardini, A. Sanna, G. Profeta, S. Massidda, Origin of the critical temperature discontinuity in superconducting sulfur under high pressure. *Phys. Rev. B* 95, 064516 (2017).
30. O. Degtyareva, E. Gregoryanz, H. K. Mao, R. J. Hemley, Crystal structure of sulfur and selenium at pressures up to 160 GPa. *High Press. Res.* 25, 17-33 (2005).
31. M. Tinkham, *Introduction to Superconductivity* (McGraw-Hill, New York, ed. 2, 1996).
32. L. I. Glazman, Vortex-induced transverse voltage within thin film, *Fiz. Nizk. Temp.* 12, 688-694(1986).
33. C. Yang, Y. Liu, Y. Wang, L. Feng, Q. He, J. Sun, Y. Tang, C. Wu, J. Xiong, W. Zhang, X. Lin, H. Yao, H. Liu, G. Fernandes, J. Xu, J. M. Valles, J. Wang, Y. Li, Intermediate bosonic metallic state in the superconductor-insulator transition. *Science* 366, 1505-1509 (2019).
34. M. A. Paalanen, A. F. Hebard, R. R. Ruel, Low-temperature insulating phases of uniformly disordered two-dimensional superconductors. *Phys. Rev. Lett.* 69, 1604-1607 (1992).
35. N. Mason, A. Kapitulnik, Dissipation effects on the superconductor-insulator transition in 2D superconductors. *Phys. Rev. Lett.* 82, 5341-5344 (1999).
36. E. Bielejec, J. Ruan, W. Wu, Hard correlation gap observed in quench-condensed ultrathin beryllium. *Phys. Rev. Lett. 87*, 036801 (2001).
37. T. I. Baturina, A. Y. Mironov, V. M. Vinokur, M. R. Baklanov, C. Strunk, Localized superconductivity in the quantum-critical region of the disorder-driven superconductor-insulator transition in TiN thin films. *Phys. Rev. Lett.* 99, 257003 (2007).
38. B. Sacépé, C. Chapelier, T. I. Baturina, V. M. Vinokur, M. R. Baklanov, M. Sanquer, Disorder-Induced Inhomogeneities of the superconducting state close to the superconductor-insulator transition. *Phys. Rev. Lett.* 101, 157006 (2008).
39. B. Sacépé, T. Dubouchet, C. Chapelier, M. Sanquer, M. Ovadia, D. Shahar, M. Feigel'man, L. Ioffe, Localization of preformed Cooper pairs in disordered superconductors. *Nat. Phys.* 7, 239-244 (2011).
40. T. L. Francavilla, R. A. Hein, The observation of a transverse voltage at the superconducting transition of thin films. *IEEE Trans. Magn.* 27, 1039-1042 (1991).
41. J. Bardeen, M. J. Stephen, Theory of the motion of vortices in superconductors. *Phys. Rev.* 140, A1197-A1207 (1965).
42. Y. Akahama, H. Kawamura, Pressure calibration of diamond anvil Raman gauge to 310 GPa. *J. Appl. Phys.* 100, 043516 (2006).
43. L. J. van der Pauw, A method of measuring specific resistivity and Hall effect of discs of arbitrary shape. *Philips Res. Rep.* 13,1-9 (1958).

Figure Captions

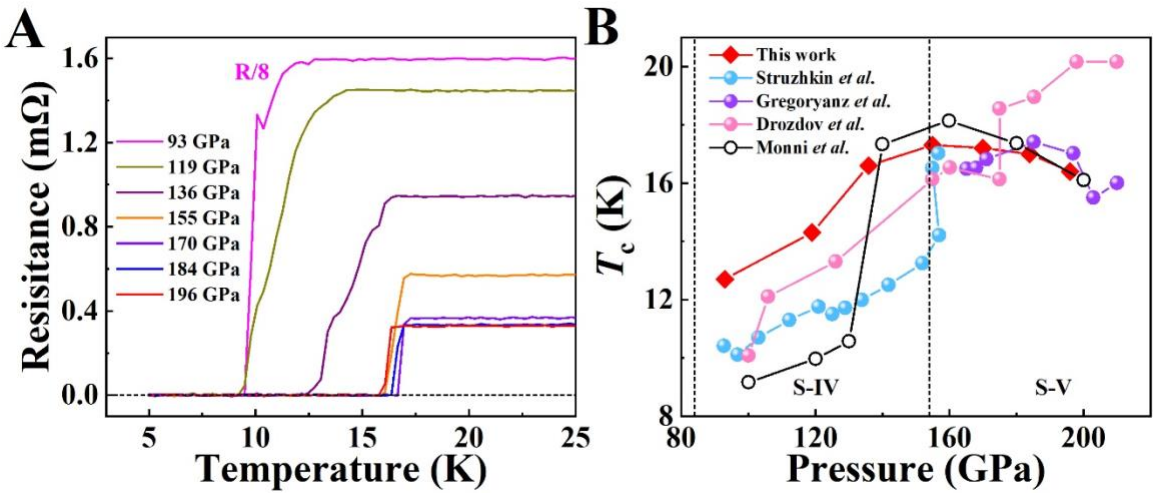

Fig. 1. Superconductivity of elemental sulfur over a wide range of pressures. (*A*) Resistance curves as a function of temperature at typical pressures (Cell_1). At low-temperature limit of the experiment, the resistance of the sample all drops to zero resistance marked by the black horizontal dotted line in the figure over the measured pressure range. Note the resistance at 93 GPa was normalized as indicated. (*B*) Dependence of the critical temperature T_c on pressure. The data represented by the rhombus, solid dots of varying colors, and hollow dots are from our measured results, previous experimental results, and previous theoretical results, respectively. The phase transition boundaries indicated by the black dotted line are derived from a previous work (30).

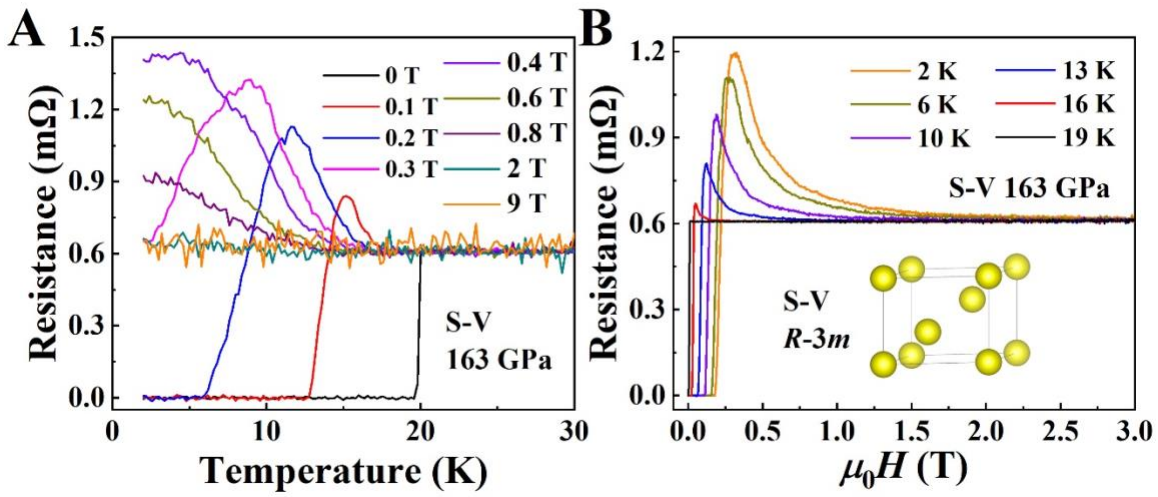

Fig. 2. Metal–bosonic insulator–superconductor transition in elemental sulfur at 163 GPa (cell_2). (*A*) Temperature dependence of electrical resistance curves under specific magnetic fields. With initial increase in magnetic field, the anomalous $R(T)$ just above T_c peak first increased, and then it was completely suppressed at about 2 T or above. The entire $R(T)$ peak shifts to lower temperature and continues to broaden with increase in field. The resistance peaks were observed in the magnetic field range from 0.1 T to nearly 2 T. The current used in the measurements is 0.001 A. (*B*) Temperature dependence of magnetic field curves at different temperatures. Increasing temperature exhibits a significant suppressive effect on the $R(H)$ peak. The inset is the crystal structure of S-V phase at 160 GPa (30). The current used in the measurements is 0.01 A.

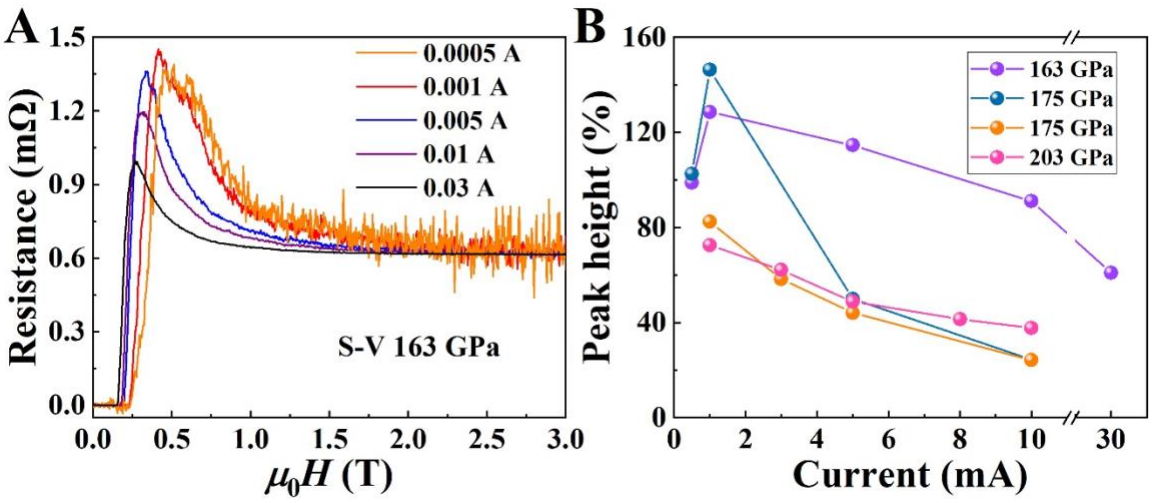

Fig. 3. The relationship between the peak value and the magnitude of the current. (*A*) Resistance curves as a function of magnetic field for different sample currents (cell_2). The increase of current first strengthens and then suppresses the peak value. The resistance peaks were observed across the entire current range (0.0005 A to 0.03 A) involved in the measurements. (*B*) Peak height vs sample current in different samples. All measurements were conducted at T=2 K.

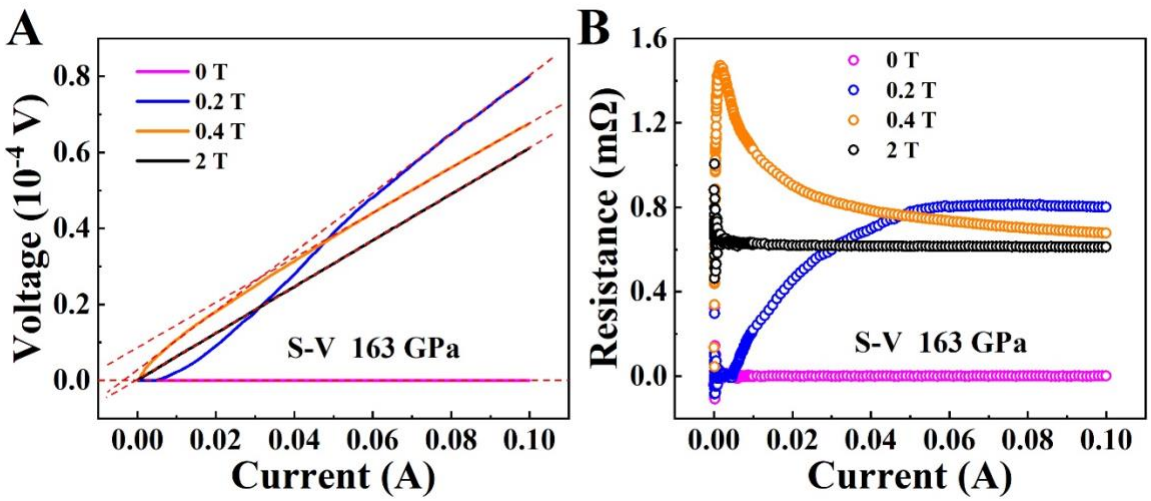

Fig. 4. Current-voltage characteristic curves (*A*) and resistance curves as a function of current (*B*) at specific magnetic field (cell_2). The red dashed lines are the linear *I-V* characteristics. As the magnetic field increases, the resistance curve gradually shows peak behavior with current, and is finally suppressed at 2 T and above. The resistance peaks were observed in the magnetic field range from 0.3 T to nearly 2 T. These measurements were all conducted at T=2 K. The pronounced fluctuations in resistance at 2 T arise from the combined influence of the strong magnetic field and the low current.

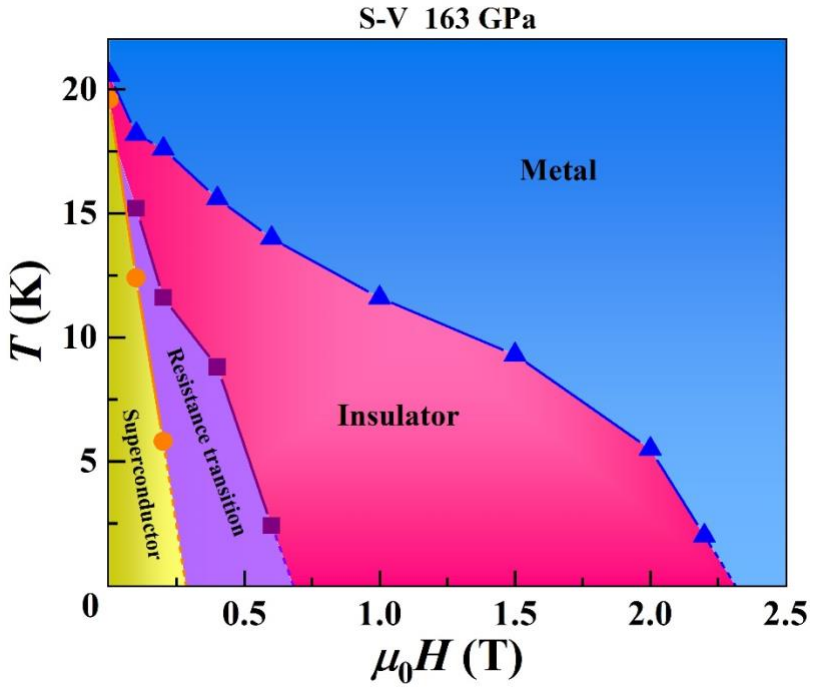

Fig. 5. Metal–bosonic insulator–superconductor phase diagram in compressed bulk sulfur. The areas of the metallic state (blue), insulating state (pink), resistance transition zone (purple), and superconducting state (yellow) are characterized by the resistance before the increase, resistance in the increase, resistance in the drop, and zero resistance, respectively. The specific method for regional division described above is presented more intuitively in the schematic diagram of Fig. S7. The blue triangles represent onset temperatures (T_c^{onset}s), the purple squares represent peak value corresponding temperature, and the orange circles represent offset temperatures (T_c^{offset}s) of the transition, where the T_c^{onset} and T_c^{offset} are defined by the point at which the extension lines that deviate from the normal state and the superconducting state, respectively. These data points were all taken from the measurements at 0.001 A.